

Scientific paper

# Effect of the Nature of the Counterions of N-alkyl Quaternary Ammonium Salts on Inhibition of the Corrosion Process<sup>†</sup>

Regina Fuchs-Godec\*

Fakulteta za kemijo in kemijsko tehnologijo Maribor, Smetanova 17, Maribor, Slovenija,  
Tel: 02-2294-443, Fax: 02-2527-774

\* Corresponding author: E-mail: fuchs@uni-mb.si

Received: 29-05-2007

<sup>†</sup>Dedicated to Prof. Dr. Jože Škerjanc on the occasion of his 70<sup>th</sup> birthday

## Abstract

Electrochemical measurements were performed to investigate the effectiveness of cationic surfactants of the N-alkyl quaternary ammonium salt type with different counterions and different chain lengths, as corrosion inhibitors for ferritic stainless steel type X4Cr13 in 2 M H<sub>2</sub>SO<sub>4</sub> solution. Two of them were single-chained surfactants and the other two were composed of three C<sub>8</sub> alkyl-chains. The chosen cationic surfactants were myristyltrimethylammonium chloride (MTACl), myristyltrimethylammonium bromide (MTABr), trioctylmethylammonium chloride (TOMACl) and trioctylmethylammonium bromide (TOMABr). Potentiodynamic polarisation measurements showed that these surfactants hinder both anodic and cathodic processes, i.e. they act as mixed-type inhibitors. It was found that the adsorption of the n-alkyl ammonium ion in 2 M H<sub>2</sub>SO<sub>4</sub> solution is in accordance with the Langmuir adsorption isotherm. Plots of log [θ/(1-θ)] vs. log c<sub>inch</sub> yielded straight lines with a slope which drastically changed at the CMC values of used surfactants. The plot of log θ vs. log c<sub>inh</sub> confirms 'the four-region' reverse orientation model of adsorption, suggested by Somasundaran and Fuerstenau. In *region IV*, where the formation of a multilayer is in progress, it is supposed that two different multilayers formed on metal surface in the case of TOMABr and MTABr. The influence of added -CH<sub>2</sub> groups (chain length) on the inhibition efficiency is greater than the influence of different counterions.

**Keywords:** Cationic surfactants, corrosion inhibitors, counterions, sulphuric acid, critical micelle concentration

## 1. Introduction

The cost of corrosion has been reported to be of the order of 1 to 5% of the GNP for many countries. Corrosion never stops, but its scope and severity can be lessened. Therefore, inhibition of corrosion is clearly very important. In that sense, use of surfactants as inhibitors is one of the best-known methods of corrosion protection, especially against corrosion in the acid pickling bath.<sup>1,2</sup> Surfactants, when used as inhibitors, act through a process of surface adsorption. Adsorption of surfactant on solid surfaces can modify the surface charge, and also the hydrophobic and other key properties of the solid surface that influence interfacial processes. In general adsorption is governed by different types of forces, such as covalent bonding, electrostatic attraction, hydrogen bonding, etc.<sup>3</sup> The adsorption of surfactants at the solid-liquid interface

is strongly influenced by a number of factors: i) the nature of the structural groups on the solid surface, for example, whether the surface contains charged sites, and the nature of the atoms of which these sites or groups are constituted; ii) the molecular structure of the surfactant being adsorbed (ionic or non-ionic), the length of the hydrophobic group and also whether it is straight-chain or branched, aliphatic or aromatic; and iii) the environment of the aqueous phase; that is its pH, electrolyte content, the presence of additives and the temperature. Altogether these factors determine the mechanism by which adsorption occurs, and the efficiency and effectiveness of adsorption.<sup>4</sup> The most accepted form of adsorption of inhibitors at metal/ solution interfaces is the formation of electrostatic (physisorption) or covalent bonding (chemisorption) between the metal surface atoms and the attractive charged parts of the adsorbents (surfactants). Several stu-

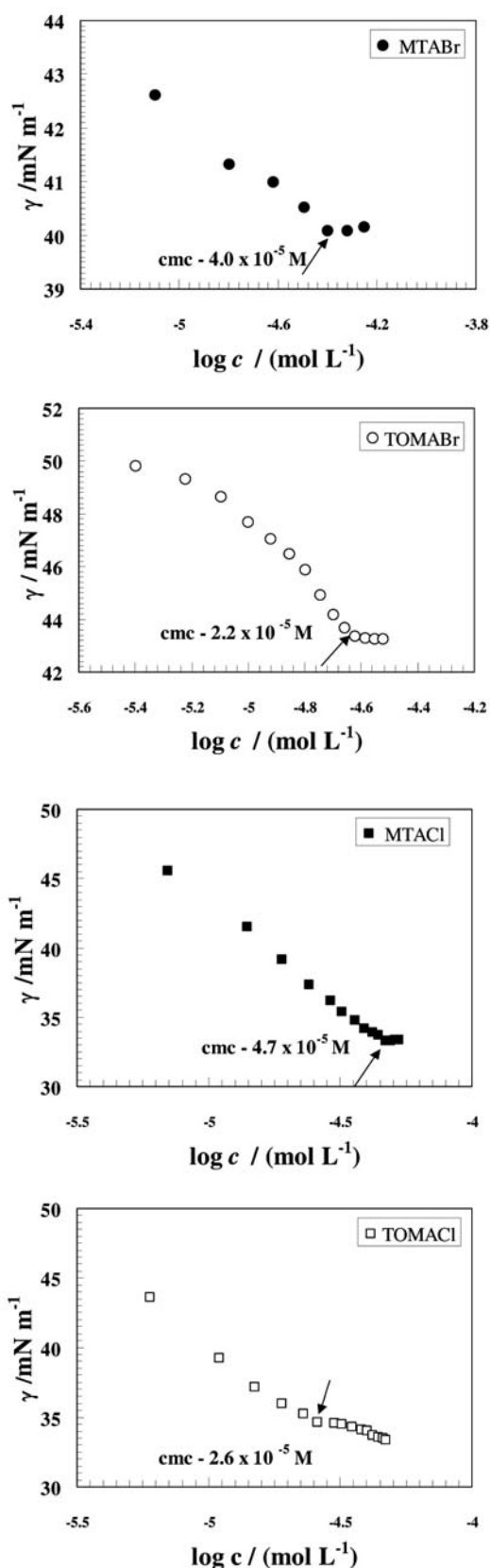
dies suggested that most organic inhibitors are adsorbed on the metal surface by displacing water molecules from the surface and forming a compact barrier film.<sup>5</sup> The ability of a surfactant molecule to adsorb is generally directly related to its ability to aggregate and to form micelles. Consequently, the critical micelle concentration (CMC) is a key indicator in determining the effectiveness of a surfactant as a corrosion inhibitor. Below the CMC, individual surfactant molecules or monomers tend to adsorb on exposed interfaces, so interfacial aggregation reduces surface tension and is related to corrosion inhibition. Above the CMC, the surface becomes covered with more than one monolayer. Thus any additional surfactant added to the solution above the CMC will lead to the formation of micelles or multiple adsorbed layers on the surface. Consequently, the surface tension, and also the corrosion current density, are not altered significantly above the CMC. Therefore, an efficient surfactant inhibitor is the one that aggregates or adsorbs at low concentrations. Generally, the lower the CMC (critical micelle concentration) the surfactant has, the greater is its tendency to adsorb at the solid surface.<sup>6–13</sup>

The CMC is a physical property of a surfactant that is influenced by a number of factors depending on the nature of the surfactant and the aqueous environment. The ionic strength of the solution is one of these factors, being responsible for the shift of the CMC value with respect to its primary value in pure water.<sup>14–16</sup> Among other properties which depend on the nature of the surfactant and also have an effect on the CMC value, is the length of the alkyl chain, and the nature of the counterions in the case when ionic surfactants are used.<sup>11, 22–24</sup>

In this investigation we studied the effectiveness of cationic surfactants of the N-alkyl quaternary ammonium salt type with different counterions and different chain lengths as corrosion inhibitors of ferritic stainless steel type X4Cr13 in 2 M H<sub>2</sub>SO<sub>4</sub> solution. Two of them were single-chained surfactants and the other two were composed of three C<sub>8</sub> alkyl-chains. The chosen cationic surfactants were myristyltrimethylammonium chloride (MTACl), myristyltrimethylammonium bromide (MTABr), trioctylmethylammonium chloride (TOMACl) and trioctylmethylammonium bromide (TOMABr).

## 2. Experimental

Electrochemical experiments were performed in a conventional three-electrode configuration. All the potentials were measured against a saturated calomel electrode (SCE) and the counter electrode was made from Pt. In all experiments electrochemical polarization was started 30 min after the working electrode was immersed in solution, to allow stabilization of the stationary potential. Before each measurement, the sample was cathodically polarized at –1.0 V (SCE) for 10 min and then allowed to reach a stable open-circuit potential which was attained in about



Figs. 1: Variation of surface tension with the concentration of MTACl, MTABr, TOMACl in TOMABr in 2.0 M H<sub>2</sub>SO<sub>4</sub> at 25 °C.

30 min. The potentiodynamic current potential curves were recorded by automatically changing the electrode potential from  $-0.7$  V to  $0.9$  V (SCE) at a scanning rate of  $2 \text{ mV s}^{-1}$ . All the experiments were performed at a temperature of  $(25 \text{ }^\circ\text{C} \pm 1)$   $^\circ\text{C}$  in non-deaerated solutions. A SOLATRON 1287 Electrochemical Interface was used to apply and control the potential. The data were collected using CorrWare and interpreted with CorrView software. The software was developed by Scribner Associates, Inc. The working electrode was ferritic stainless steel of type X4Cr13. The test specimens were fixed in a PTFE holder, and the geometric area of the electrode exposed to electrolyte was  $0.785 \text{ cm}^2$ . The metal surface was hand polished successively with emery papers of grade 400, 600, 800, 1000 and 1200. Next, the specimen was fine polished with diamond paste to obtain a mirror finish surface. After polishing, the working electrode was washed with ethanol, rinsed several times with distilled water and finally dried with hot air.

The chosen cationic surfactants were Fluka products of pure quality ( $>97\%$ ) and used without further purification. Table 1 lists the structural formula together with its molecular weight.

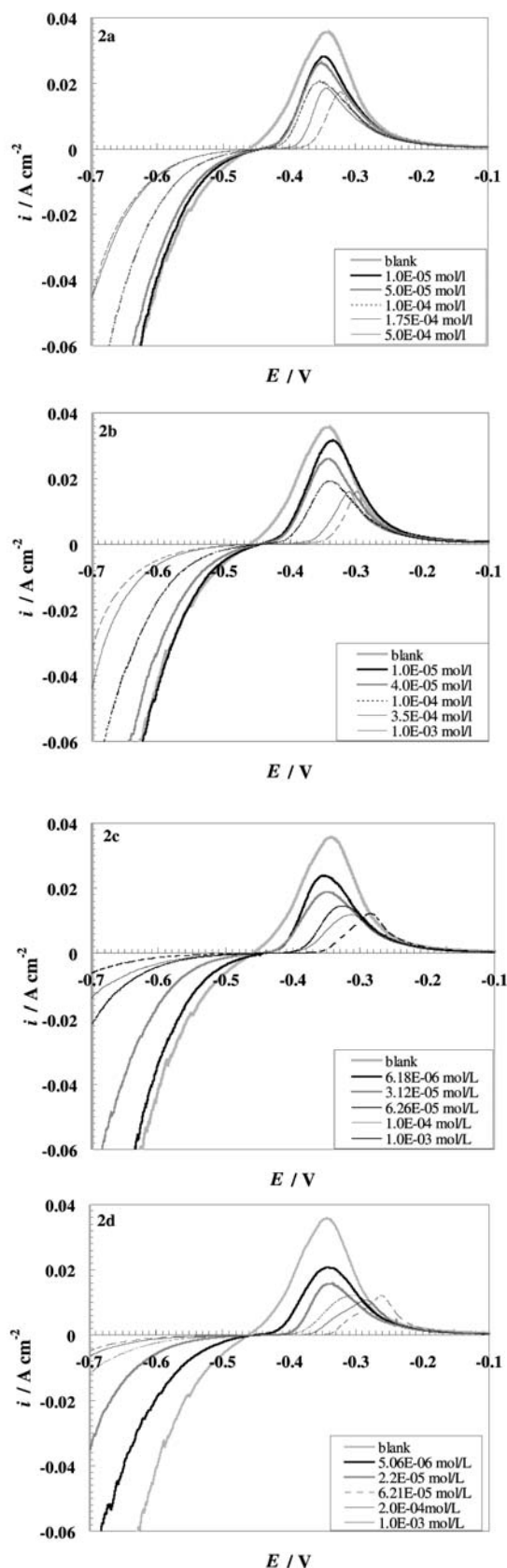
**Table 1:** Basic characteristics of the surfactants used in this study.

Surfactant	Structural formula	Molecular weight
MTACl	$\text{CH}_3(\text{CH}_2)_{13}\text{N}(\text{Cl})(\text{CH}_3)_3$	291.95
MTABr	$\text{CH}_3(\text{CH}_2)_{13}\text{N}(\text{Br})(\text{CH}_3)_3$	336.41
TOMACl	$[\text{CH}_3(\text{CH}_2)_6\text{CH}_2]_3\text{N}(\text{Cl})\text{CH}_3$	404.17
TOMABr	$[\text{CH}_3(\text{CH}_2)_6\text{CH}_2]_3\text{N}(\text{Br})\text{CH}_3$	448.62

All solutions were prepared using water obtained from a Millipore Super-Q system. The surface tension of the surfactant solutions containing  $2 \text{ mol L}^{-1} \text{ H}_2\text{SO}_4$  was measured with a Krüss-K12 processor tensiometer with a plate at  $25 \text{ }^\circ\text{C}$ . The surface tension was measured until the equilibrium value was reached (Figs. 1a-c). The values obtained for the CMC of the *n*-alkyl quaternary ammonium salts in  $2.0 \text{ M H}_2\text{SO}_4$  were  $(4.0 \pm 0.8 \times 10^{-5}) \text{ M}$  for MTABr,  $(4.7 \pm 0.3 \times 10^{-5}) \text{ M}$  for MTACl,  $(2.2 \pm 0.2 \times 10^{-5}) \text{ M}^{25}$  for TOMABr and  $(2.6 \pm 0.2 \times 10^{-5}) \text{ M}$  for TOMACl<sup>25</sup> (Figs. 1)

### 3. Results and Discussion

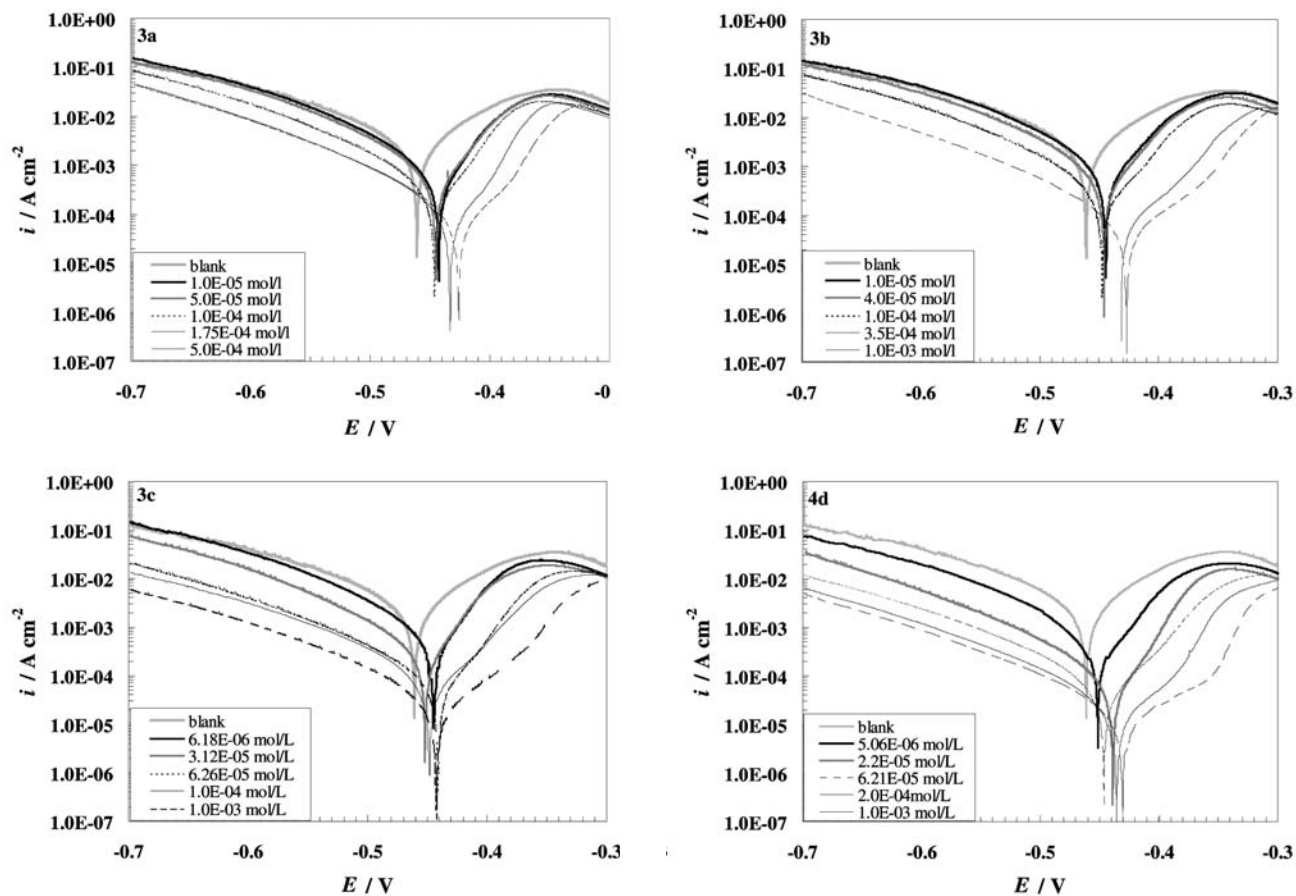
The effect of single-chained surfactants and surfactants composed of three  $\text{C}_8$  alkyl-chains on the current-potential characteristics as given by the polarisation curves for ferritic stainless steel type X4Cr13 in  $2 \text{ M H}_2\text{SO}_4$  is presented in Figs. 2 and 3. A noticeable decrease of the anodic current peak, and also an appreciable lowering of the cathodic current may be observed from these figures. This result suggests that addition of the se-



**Figs. 2:** Potentiodynamic polarisation curves ( $2 \text{ mVs}^{-1}$ ) for stainless steel X4Cr13 in  $2.0 \text{ M H}_2\text{SO}_4$  at various concentrations of (a) MTACl, (b) MTABr, (c) TOMACl and (d) TOMABr at  $25 \text{ }^\circ\text{C}$ .

**Table 2:** Kinetic parameters for corrosion of stainless steel X4Cr13 obtained from potentiodynamic polarisation curves in 2.0 M H<sub>2</sub>SO<sub>4</sub> at various concentrations of MTACl, MTABr, TOMACl and TOMABr at 25 °C.

2.0 M H <sub>2</sub> SO <sub>4</sub> + x M MTACl	$i_{\text{corr}} /$ (Acm <sup>-2</sup> )	$E_{\text{corr}} /$ (V vs. NKE)	$R_p /$ (Ωcm <sup>-2</sup> )	$Q_a /$ (Ccm <sup>-2</sup> )	$\theta_{\text{corr}}$	$\theta_{R_p}$	$\theta_{Q_a}$
0.0	9.96 × 10 <sup>-4</sup>	-0.461	15.6	2.121			
1.00 × 10 <sup>-5</sup>	8.01 × 10 <sup>-4</sup>	-0.449	19.77	1.477	0.196	0.211	0.303
2.00 × 10 <sup>-5</sup>	7.62 × 10 <sup>-4</sup>	-0.447	20.68	1.420	0.235	0.246	0.330
3.00 × 10 <sup>-5</sup>	7.37 × 10 <sup>-4</sup>	-0.441	20.98	1.415	0.260	0.256	0.333
<b>5.00 × 10<sup>-5</sup></b>	<b>6.96 × 10<sup>-4</sup></b>	<b>-0.445</b>	<b>22.39</b>	<b>1.403</b>	<b>0.301</b>	<b>0.303</b>	<b>0.338</b>
7.00 × 10 <sup>-5</sup>	5.45 × 10 <sup>-4</sup>	-0.444	31.42	1.090	0.453	0.503	0.485
1.00 × 10 <sup>-4</sup>	3.70 × 10 <sup>-4</sup>	-0.443	45.00	0.996	0.628	0.650	0.530
2.50 × 10 <sup>-4</sup>	1.68 × 10 <sup>-4</sup>	-0.437	102.07	0.846	0.831	0.847	0.601
5.00 × 10 <sup>-4</sup>	1.41 × 10 <sup>-4</sup>	-0.424	122.50	0.806	0.858	0.872	0.620
1.00 × 10 <sup>-3</sup>	9.74 × 10 <sup>-5</sup>	-0.418	153.44	0.694	0.902	0.898	0.672
2.0 M H <sub>2</sub> SO <sub>4</sub> + x M MTABr	$i_{\text{corr}} /$ (Acm <sup>-2</sup> )	$E_{\text{corr}} /$ (V vs. NKE)	$R_p /$ (Ωcm <sup>-2</sup> )	$Q_a /$ (Ccm <sup>-2</sup> )	$\theta_{\text{corr}}$	$\theta_{R_p}$	$\theta_{Q_a}$
0.0	9.96 × 10 <sup>-4</sup>	-0.461	15.6	2.121			
1.00 × 10 <sup>-5</sup>	7.78 × 10 <sup>-4</sup>	-0.449	19.82	1.655	0.219	0.213	0.219
2.00 × 10 <sup>-5</sup>	7.43 × 10 <sup>-4</sup>	-0.447	20.75	1.554	0.253	0.248	0.267
3.00 × 10 <sup>-5</sup>	7.27 × 10 <sup>-4</sup>	-0.446	21.44	1.427	0.270	0.272	0.327
<b>4.00 × 10<sup>-5</sup></b>	<b>7.14 × 10<sup>-4</sup></b>	<b>-0.446</b>	<b>22.88</b>	<b>1.393</b>	<b>0.283</b>	<b>0.318</b>	<b>0.343</b>
5.00 × 10 <sup>-5</sup>	6.23 × 10 <sup>-4</sup>	-0.447	27.99	1.183	0.374	0.442	0.442
1.00 × 10 <sup>-4</sup>	3.23 × 10 <sup>-4</sup>	-0.442	46.05	1.051	0.675	0.661	0.504
2.52 × 10 <sup>-4</sup>	1.25 × 10 <sup>-4</sup>	-0.425	150.46	0.676	0.874	0.896	0.681
3.50 × 10 <sup>-4</sup>	1.04 × 10 <sup>-4</sup>	-0.433	158.88	0.667	0.895	0.902	0.685
5.00 × 10 <sup>-4</sup>	8.64 × 10 <sup>-5</sup>	-0.420	220.93	0.559	0.913	0.929	0.736
1.00 × 10 <sup>-3</sup>	5.62 × 10 <sup>-5</sup>	-0.425	252.66	0.549	0.943	0.938	0.741
2.0 M H <sub>2</sub> SO <sub>4</sub> + x M TOMACl	$i_{\text{corr}} /$ (Acm <sup>-2</sup> )	$E_{\text{corr}} /$ (V vs. NKE)	$R_p /$ (Ωcm <sup>-2</sup> )	$Q_a /$ (Ccm <sup>-2</sup> )	$\theta_{\text{corr}}$	$\theta_{R_p}$	$\theta_{Q_a}$
0.0	9.96 × 10 <sup>-4</sup>	-0.461	15.6	2.121			
6.18 × 10 <sup>-6</sup>	7.16 × 10 <sup>-4</sup>	-0.449	22.45	1.321	0.281	0.305	0.376
1.00 × 10 <sup>-5</sup>	6.66 × 10 <sup>-4</sup>	-0.446	25.013	/	0.337	0.376	/
1.65 × 10 <sup>-5</sup>	5.90 × 10 <sup>-4</sup>	-0.447	29.94	1.271	0.407	0.479	0.400
2.65 × 10 <sup>-5</sup>	5.10 × 10 <sup>-4</sup>	-0.447	32.278	1.214	0.487	0.517	0.427
<b>3.12 × 10<sup>-5</sup></b>	<b>4.44 × 10<sup>-4</sup></b>	<b>-0.446</b>	<b>40.491</b>	<b>1.119</b>	<b>0.554</b>	<b>0.615</b>	<b>0.472</b>
6.21 × 10 <sup>-5</sup>	2.50 × 10 <sup>-4</sup>	-0.446	64.011	0.796	0.746	0.756	0.624
8.07 × 10 <sup>-5</sup>	1.91 × 10 <sup>-4</sup>	-0.445	79.483	0.689	0.808	0.804	0.674
1.00 × 10 <sup>-4</sup>	1.49 × 10 <sup>-4</sup>	-0.440	167.47	0.646	0.850	0.907	0.695
2.00 × 10 <sup>-4</sup>	8.42 × 10 <sup>-5</sup>	-0.438	278.55	0.602	0.915	0.944	0.716
5.00 × 10 <sup>-4</sup>	3.93 × 10 <sup>-5</sup>	-0.432	408.22	0.559	0.960	0.961	0.736
1.00 × 10 <sup>-3</sup>	1.83 × 10 <sup>-5</sup>	-0.434	623.76	0.527	0.981	0.975	0.751
2.0 M H <sub>2</sub> SO <sub>4</sub> + x M TOMABr	$i_{\text{corr}} /$ (Acm <sup>-2</sup> )	$E_{\text{corr}} /$ (V vs. NKE)	$R_p /$ (Ωcm <sup>-2</sup> )	$Q_a /$ (Ccm <sup>-2</sup> )	$\theta_{\text{corr}}$	$\theta_{R_p}$	$\theta_{Q_a}$
0.0	9.96 × 10 <sup>-4</sup>	-0.461	15.6	2.121			
6.00 × 10 <sup>-6</sup>	3.00 × 10 <sup>-4</sup>	-0.447	49.31	1.108	0.699	0.684	0.477
1.00 × 10 <sup>-5</sup>	2.33 × 10 <sup>-4</sup>	-0.444	70.82	1.001	0.760	0.780	0.528
1.65 × 10 <sup>-5</sup>	1.94 × 10 <sup>-4</sup>	-0.444	86.76	0.921	0.805	0.820	0.566
<b>2.20 × 10<sup>-5</sup></b>	<b>1.49 × 10<sup>-4</sup></b>	<b>-0.443</b>	<b>96.50</b>	<b>0.905</b>	<b>0.827</b>	<b>0.838</b>	<b>0.573</b>
3.12 × 10 <sup>-5</sup>	1.07 × 10 <sup>-4</sup>	-0.440	140.26	0.857	0.893	0.888	0.595
6.21 × 10 <sup>-5</sup>	5.56 × 10 <sup>-5</sup>	-0.440	278.00	0.682	0.944	0.944	0.678
8.07 × 10 <sup>-5</sup>	3.92 × 10 <sup>-5</sup>	-0.435	557.92	0.569	0.961	0.972	0.731
1.00 × 10 <sup>-4</sup>	2.67 × 10 <sup>-5</sup>	-0.432	606.90	0.537	0.973	0.974	0.746
1.30 × 10 <sup>-4</sup>	1.78 × 10 <sup>-5</sup>	-0.431	725.79	0.532	0.982	0.978	0.749
2.00 × 10 <sup>-4</sup>	1.74 × 10 <sup>-5</sup>	-0.433	745.10	0.531	0.983	0.979	0.749
5.00 × 10 <sup>-4</sup>	1.62 × 10 <sup>-5</sup>	-0.429	869.86	0.525	0.984	0.982	0.752
1.00 × 10 <sup>-3</sup>	1.45 × 10 <sup>-5</sup>	-0.427	1036.6	0.465	0.985	0.985	0.780



Figs. 3: Influence of the added surfactants (a) MTACl, (b) MTABr, (c) TOMACl and (d) TOMABr on the cathodic and the anodic behaviour of stainless steel X4Cr13 in 2 M  $\text{H}_2\text{SO}_4$  at 25 °C

lected cationic surfactants reduces anodic dissolution, and retards the hydrogen evolution reaction. This phenomenon became more expressed with increase in the surfactant concentration.

The shift of  $E_{\text{corr}}$  towards a more noble value, and to an order of magnitude lower corrosion current density  $i_{\text{corr}}$  with respect to the inhibitor-free solution (Figs. 3) was observed. It should be mentioned that for surfactant concentrations around the CMC values, the voltammograms in Figs. 2 had flat profiles with a minimal value of the current density. The flat portion extended to about 100 mV in both direction with regard to the corrosion potential of the 2 M  $\text{H}_2\text{SO}_4$  solution in the absence of inhibitors ( $-0.461$  V vs. SCE). Within this potential region, a high value of the inhibition efficiency was expected. In Fig. 3 we also see that for concentrations higher than the CMC values, the phenomenon denoted as a “dual-current plateau” appears in the range of  $-425$  to  $-370$  mV/SCE. Here two different anodic slopes were obtained. Finally, it seems that for overvoltages higher than  $-200$  mV/SCE, the presence of the surfactants investigated in this study did not change the current versus potential characteristics (Fig. 2), since there was no further change in the polarisation curves. These results also show that the inhibition process (for

these inhibitors) to a great extent depends on the electrode potential.

The most important kinetic parameters of corrosion are: (i) the corrosion current density ( $i_{\text{corr}}$ ), (ii) the polarisation resistance ( $R_p$ ), and (iii) the charge involved in the surface anodic reaction ( $Q_a$ ). The polarisation resistance was obtained by linear polarisation within the potential range of  $\pm 10$  mV with respect to  $E_{\text{corr}}$  and the charge by integration of the area under the  $i$ - $E$  curve. Extrapolation of the Tafel line allowed calculation of the corrosion current density ( $i_{\text{corr}}$ ). These parameters were determined simultaneously by the computer (CorrView software). The corrosion parameters obtained for X4Cr13 stainless steel as a function of the concentration of the cationic surfactants are given in Table 2.

### 3. 1. Adsorption isotherm

The surface coverage,  $\theta$ , was calculated via the kinetic parameters measured during the corrosion processes, that is the polarisation resistance ( $R_p$ ), the corrosion current density ( $i_{\text{corr}}$ ) and the charge ( $Q_a$ ) involved in the surface anodic reaction (cf Equations 1a and 1b). In the case of the polarisation resistance,  $\theta$  was calculated via Equation (1a).

Equation (1b) was used in connection with the corrosion current density, and the charge involved in the surface anodic reaction ( $Q_a$ ), was obtained from the electrochemical measurements, where  $x = i_{\text{corr}}$  or  $Q_a$ . The notation  $R_p$ ,  $i_{\text{corr}}$ ,  $Q_a$  was used for measurements without added surfactants, and the primed quantities  $R_p'$ ,  $i_{\text{corr}}'$ ,  $Q_a'$  apply when surfactants were added to the solution of 2.0 M  $\text{H}_2\text{SO}_4$ .

$$\theta = \frac{R_p' - R_p}{R_p'} \quad (1a)$$

$$\theta = \frac{x - x'}{x} \quad (1b)$$

We attempted to fit  $\theta$  values with standard adsorption isotherms, including those of Frumkin, Flory-Huggins, Temkin, and also by the Langmuir-type adsorption isotherm. It was found that the experimental results for all four cationic surfactants of the N-alkyl quaternary ammonium salt type can be fitted quite well with the Langmuir adsorption isotherm expressed as

$$\frac{\theta}{1-\theta} = Kc \quad (2)$$

or

$$\frac{c}{\theta} = \frac{1}{K} + c \quad (3)$$

In the expressions above  $c$  is the concentration of inhibitor. Further,  $K$  is the modified adsorption equilibrium constant, related to the free energy of adsorption  $\Delta G_{\text{ads}}$  by:

$$K = \frac{1}{c_{\text{solvent}}} \exp\left(\frac{-\Delta G_{\text{ads}}}{RT}\right) \quad (4)$$

where  $c_{\text{solvent}}$  is the molar concentration of solvent, which in the case of water is  $55.5 \text{ mol L}^{-1}$ . The adsorption

isotherms are plotted in Fig. 4. The relations  $c/\theta$  versus  $c$  are linear, with the slopes close to unity for all four investigated cationic surfactants, as required by Eq. 3.

The logarithmic forms of Eqs. 2 and 4 are:

$$\log c_{\text{inh}} = \log\left(\frac{\theta}{1-\theta}\right) - \log K \quad (5)$$

$$\log K = -1.74 - \left(\frac{-\Delta G_{\text{ads}}}{2.303RT}\right) \quad (6)$$

Figures 5 a–b show  $\log [\theta/(1-\theta)]$  against the logarithm of the added surfactant concentration with  $\theta$  calculated from Equation 1a. All the curves look similar; the slope changes at a certain concentration of added surfactant. The first intersection of the straight lines is at exactly  $c = 3.0 \times 10^{-5} \text{ M}$ , and  $5 \times 10^{-5} \text{ M}$  for TOMACl and MTACl,<sup>25</sup> respectively,  $2.2 \times 10^{-5} \text{ M}$  for TOMABr and  $4.0 \times 10^{-5} \text{ M}$  for MTABr. These values represent the CMC values of the cationic surfactants under study in 2.0 M  $\text{H}_2\text{SO}_4$ . The results are in good agreement with surface tension measurements. Furthermore, from Fig. 5 we see that the triple-tailed surfactants exhibited better inhibition efficiency than the single-chain ones. For the case when a single chain is elongated, Atkin et al.<sup>22</sup> suggested the following explanation. As the hydrocarbon chain length of the surfactant molecule is increased, the monomer is rendered 'more hydrophobic'. As a consequence an increased number of 'clathrate bound' water molecules are required to solubilise successively longer tail-groups, which lowers the overall entropy of the system. As a result, the surfactants with longer hydrocarbon chains have a much greater driving force for aggregation, which considerably reduces the CMC value. A similar explanation, invoking the hydrophobic effect, can also be used in the case when we have two or three (shorter) hydrophobic chains. It could be speculated that it is the number of  $-\text{CH}_2$  groups as a whole which determines the inhibition efficiency.

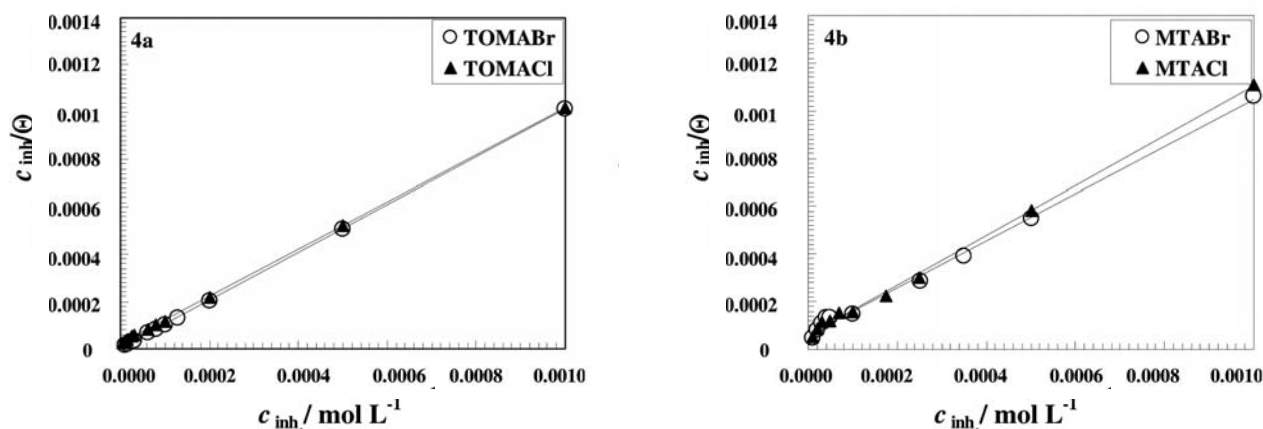


Fig. 4: Langmuir plots for; (a) TOMABr and MTABr, (b) TOMACl and MTACl in 2.0 M  $\text{H}_2\text{SO}_4 + x \text{ M } c_{\text{inh}}$  obtained from  $i_{\text{corr}}$ .

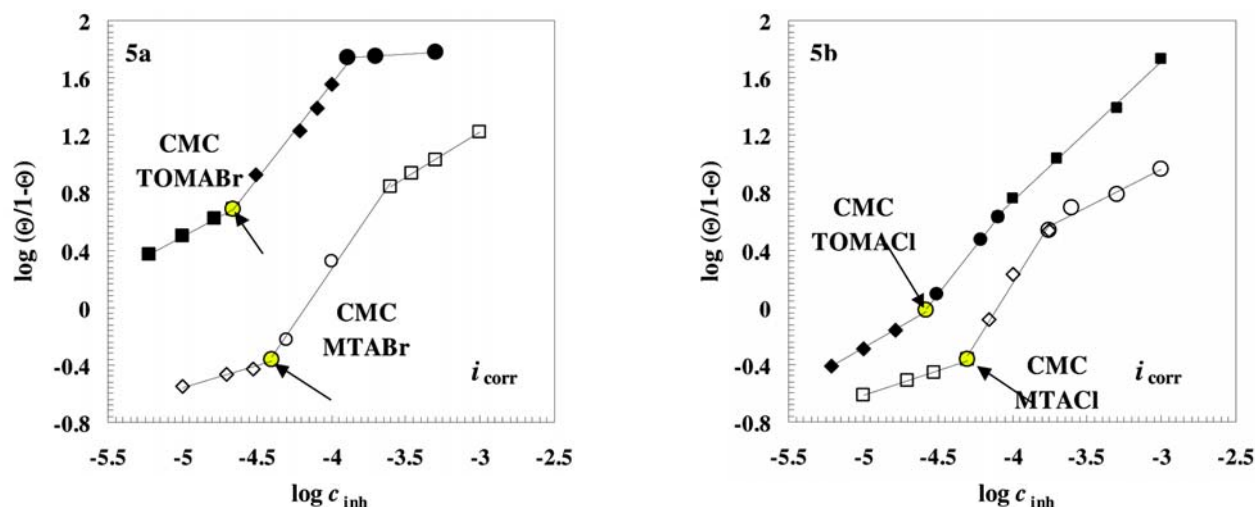


Fig. 5: Graphical determination of CMCs for: (a) TOMABr and MTABr, (b) TOMACl and MTACl. in 2.0 M H<sub>2</sub>SO<sub>4</sub> + x M c<sub>inh</sub> (θ obtained from  $i_{corr}$ ) through the Langmuir isotherm.

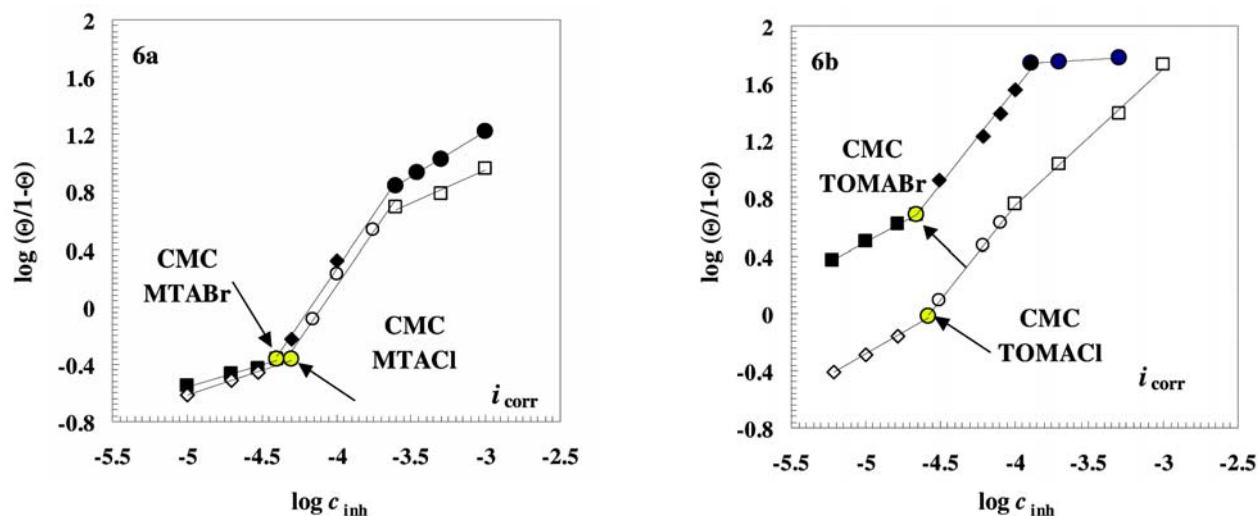


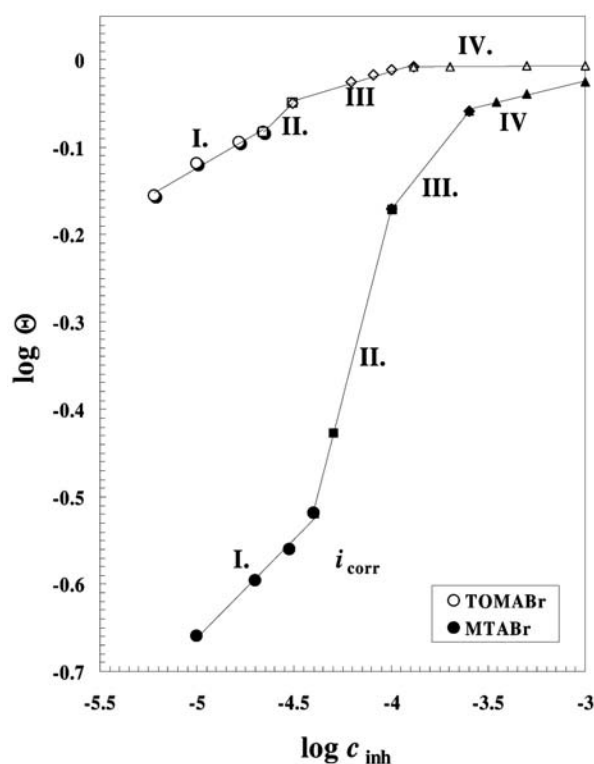
Fig. 6: Influence of the nature of the counterion on the surface coverage, θ: (a) MTABr and MTACl, (b) for TOMABr and TOMACl v 2.0 M H<sub>2</sub>SO<sub>4</sub> + x M c<sub>inh</sub> (θ was obtained  $i_{corr}$  using the Langmuir isotherm).

Fig. 6 shows the effect of the nature of the halide counterion on the surface coverage. In all measurements performed, the highest inhibition efficiencies were observed when bromide ions were used in the corrosion medium. Note that CMC values of the bromide salts are smaller a those of the corresponding chlorides. The explanation of this phenomenon is related to the differences in the hydration of the two ions. The chloride ion has a smaller crystal radius than the bromide ion. As a consequence, the chloride ion is more strongly solvated and therefore larger in solution than the bromide ion. The chloride ions retain their solvation shell in interacting with surfactant. In other words, chloride ions are less closely associated with the cationic head group of the surfactant than bromide ions, and not as effective in 'shielding' the head group charge.

This leads to greater electrostatic repulsion between the surfactant head group charges, not only within the micelle, but also between the surfactant micelles themselves.<sup>22</sup> This effect causes an increase in the CMC value and also a decrease of adsorption.

It has been suggested<sup>3,22,26,27,28</sup> that adsorption of ionic surfactants on oppositely charged surfaces occurs via the 'four-region' reverse orientation model of adsorption, as first proposed by Somasundaran and Fuerstenau.<sup>28</sup> For easier interpretation of the adsorption isotherms they used a log–log plot. The primary advantage of using such a representation is that it amplifies the features of the isotherm at low surface excess values. It was suggested that in *region I* of the isotherm, surfactant monomers are electrostatically adsorbed on the charged surface, with

head-groups in contact with the surface (see Fig.7). Hydrocarbon tail-groups may interact with hydrophobic regions of the surface. In other words, at the beginning of the adsorption process the hydrophobic chains may also be arranged horizontally. Because the adsorption of monomer molecules does not compensate fully for the surface charge, the slope of the adsorption isotherm in the second region is increased. This increase is explained by the surface aggregation *region II*. Using experimental techniques such as Raman spectroscopy, fluorescence spectroscopy, electron spin resonance and contact angle measurement, Somasundaran et al.<sup>26,29–31</sup> have shown that surfactants are adsorbed with their head-groups facing towards the surface, while the hydrocarbon tail-groups protrude into solution. This creates hydrophobic patches on the surface. *Region III* shows a slower rate of adsorption than *region II*. The transition between *regions II* and *III* is thought to be due to neutralisation of the surface charge. Finally, in *region IV*, saturation of the surface with surfactant molecules is attained, and multilayer adsorption is started.



**Figure 7:** Surface coverage,  $\theta$ , as a function of concentration of MTABr and TOMABr on a double log scale; stainless steel X4Cr13 in 2.0 M  $\text{H}_2\text{SO}_4$  at 25 °C ( $\theta$  obtained from  $i_{\text{corr}}$ ).

The effectiveness of adsorption in *region IV* (i.e. the amount adsorbed at surface saturation) may increase, decrease, or show no change, depending on the orientation of the surfactant at the metal-solution interface. If adsorption is perpendicular to the metal surface in a close packed

arrangement, an increase in the length of the straight-chain hydrophobic group appears to cause no significant change in the number of moles of surfactant adsorbed per unit area. Moreover, for perpendicular orientation of surfactant molecules the effectiveness of adsorption may also be governed by the relative size of the hydrophilic group in comparison with the hydrophobic chain. When the cross-sectional area of the hydrophilic group is greater than that of the hydrophobic chain, a smaller amount is adsorbed at saturation conditions. Finally, if the surfactant arrangement is not close-packed, though predominately perpendicular, or if the molecules are tilted away from the perpendicular orientation, adsorption may be stronger.<sup>4</sup> Marques et al.<sup>32</sup> reported that double-tailed cationic surfactants form bilayer-type assemblies, such as vesicles or lamellae. Symmetric double-chained cationic surfactants have very low solubility in water, due to the strong hydrophobicity associated with the two-alkyl chains.<sup>33,34</sup>

On the basis of the ‘four-region’ reverse orientation model of adsorption, and the results of Marques,<sup>32</sup> it can be assumed that the multilayer of TOMABr has the same perpendicular orientation as is formed in the second and third regions. This means that the molecules form the close packed arrangement as shown on Figure 8a. Additionally, from Fig. 7 it may be seen, that no significant change in the adsorption effectiveness is observable in this region. In contrast to this, the other surfactant MTABr shows slightly increased adsorption effectiveness at saturation. It can be speculated that the multilayer of MTABr is arranged predominately perpendicularly, though not in the close-packed structure, but perhaps as semi spherical caps as shown schematically in Figure 8b.

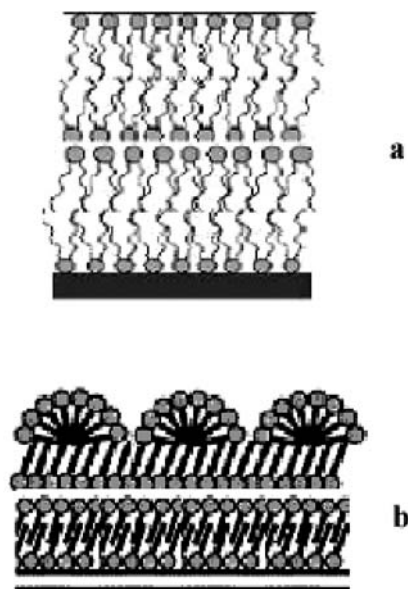
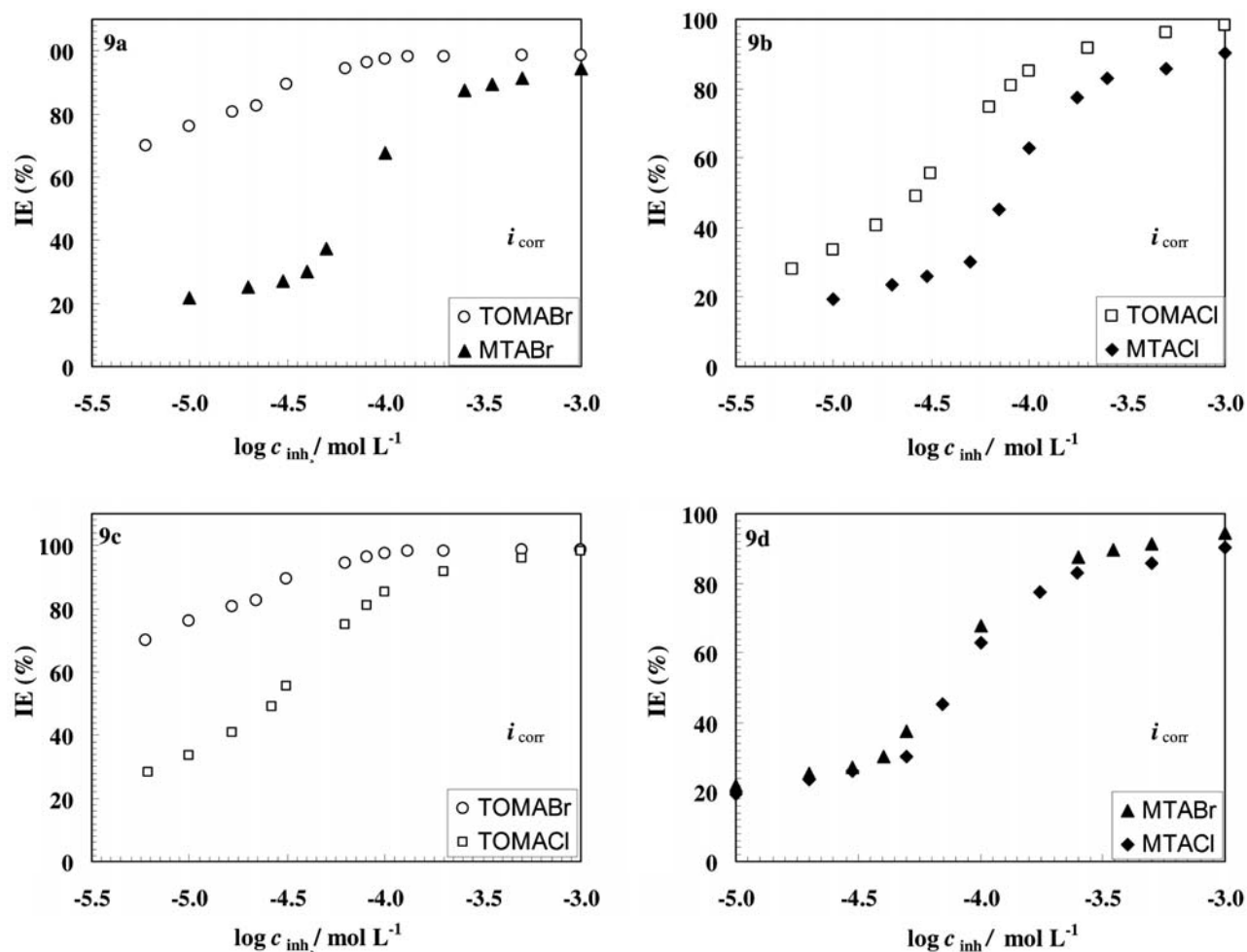


**Figure 8:** Schematic representation of the assumed structure of the multilayer in *region IV* where saturation of the surface with surfactant molecules is attained; a) for TOMABr (triple-chained) b) for MTABr (single-chained).



**Figs. 9a–d:** Inhibition efficiency as a function of concentration of added MTACl, MTABr, TOMACl and TOMABr in 2.0 M  $\text{H}_2\text{SO}_4$ . ( $\theta$  obtained from  $i_{corr}$ ); a–b (influence of the number of  $-\text{CH}_2$  groups), c–d (influence of the type of counterion)

Figure 9 shows the corrosion inhibition efficiency ( $\text{IE} = \theta \times 100$ ) for all four selected cationic surfactants in 2.0 M  $\text{H}_2\text{SO}_4$ . On Figs. 9a and b, the influence of the number of  $-\text{CH}_2$  groups on IE is visible, whereas on Figs. 9c and d, the influence of the nature of the halide counterion ( $\text{Cl}^-$  or  $\text{Br}^-$ ) on the inhibition efficiency of N-alkyl quaternary ammonium salts is presented. On the basis of the plots in Fig. 9, we can conclude that the total number of  $-\text{CH}_2$  groups in the alkyl chains has a stronger influence on the inhibition efficiency than the effect of the nature of the counterion. In other words, the hydrophobic ‘interaction’ is, under these conditions, more important than the ion-specific effects.

Values of the free energy of adsorption  $\Delta G_{ads}$  were calculated from Fig. 5 and collected in Table 3. All values of  $\Delta G_{ads}$  are negative, thus suggesting the spontaneity of the adsorption process.  $\Delta G_{ads}$  becomes more negative when the concentration of added surfactant is above the CMC. This is due to micelle formation; the micelles are highly charged, which increases the adsorption, and consequently reduces the corrosion rate. Additionally, in the

case when TOMABr and TOMACl are used, the corresponding values for  $\Delta G_{ads}$  become noticeably more negative already at a concentration that is lower than their CMCs in comparison with MTABr and MTACl. This result is consistent with our conclusion that the total number of  $-\text{CH}_2$  groups in the alkyl chain is a more important factor than the type of counterion in the investigated corrosion system.

**Table 3:** Calculated values of  $\Delta G_{ads}$  (from the Langmuir isotherm) below and above the CMC, for MTACl, MTABr, TOMACl and TOMABr in 2.0 M  $\text{H}_2\text{SO}_4$ .

Surfactant	$\Delta G_{ads} / \text{kJ mol}^{-1}$	
	below CMC	above CMC
<b>MTACl</b>	-16.472	-45.289
<b>MTABr</b>	-15.295	-46.278
<b>TOMACl</b>	-25.752	-44.541
<b>TOMABr</b>	-28.587	-48.905

## 4. Conclusions

Ionic surfactants of the N-alkyl quaternary ammonium salt type showed good inhibitory properties for stainless steel type X4Cr13 in aqueous solutions of 2 mol L<sup>-1</sup> H<sub>2</sub>SO<sub>4</sub>.

Surfactants having bromide as counterion acted as better corrosion inhibitors. They provide higher IE at the same concentration in comparison with the chloride salts. The bromide ion is known to release water more easily than the chloride ion. This leads to an increase of the shielding effect of the head groups of the surfactant in the presence of bromide. This effect causes a somewhat weaker electrostatic repulsion between the head group within the micelle and also between them. All these effects contribute to stronger adsorption and consequently to more efficient inhibition.

The surface coverage  $\theta$  was calculated on the basis of the corrosion parameters ( $R_p$ ,  $i_{\text{corr}}$ ,  $Q_a$ ) and it was found that it could be represented by the Langmuir isotherm.

The plot of  $\log \theta$  vs.  $\log c_{\text{inh}}$  confirms 'the four-region' reverse orientation model of adsorption, suggested by Somasundaran and Fuerstenau. In region IV, where saturation of the surface with surfactant molecules is attained and the formation of a multilayer starts, a difference between TOMABr (triple-chain C<sub>8</sub>) and MTABr (C<sub>14</sub> single chain) was observed.

In all measurements performed, higher inhibition efficiencies were observed when the concentration of surfactant exceeded its CMC. The influence of the number -CH<sub>2</sub> groups (chain length) on the IE is stronger than effects associated with the nature of the counterion in solution.

## 5. References

1. T. B. Du, J. J. Chen, D. Z. Cao, *J. Mater. Sci.* **2001**, *36*, 3903–3907.
2. T. Y. Soror, M. A. El-Ziady, *Mater. Chem. & Phys.* **2002**, *77*, 697–703.
3. R. Zhang, P. Somasundaran, *Adv. Colloid & Interface Sci.* **2006**, *123–126*, 213–229.
4. M. J. Rosen, *Surfactants and Interfacial Phenomena*, 2<sup>nd</sup> ed., Wiley-VCH, New York 1989, 33–202.
5. M. El Azhar, B. Mernari, M. Traisnel, F. Bentiss, M. Lagrenée, *Corros. Sci.* **2001**, *43*, 2229–2238.
6. M. A. Migahed, *Mater. Chem. & Phys.* **2005**, *93*, 48–53.
7. F. Bentiss, M. Traisnel, M. Lagrenée, *Corros. Sci.* **2000**, *42*, 127–146.
8. F. Bentiss, M. Lebrini, M. Lagrenée, *Corros. Sci.* **2005**, *47*, 2915–2931.
9. S. T. Keera, M. A. Deyab, *Colloids Surf. A.* **2005**, *266*, 129–140.
10. S. Paria, K. C. Khilar, *Adv. Colloid & Interface Sci.* **2004**, *110*, 75–95.
11. V. Branzoi, F. Branzoi, M. Baibarac, *Mater. Chem. & Phys.* **2000**, *65*, 288–297.
12. R. Atkin, V. S. J. Craig, E. J. Walness, S. Biggs, *J. Coll. and Interface Sci.* **2003**, *266*, 236–244.
13. A. Popova, M. Christov, S. Raicheva, E. Sokolova, *Corros. Sci.* **2004**, *46*, 1333–1350.
14. S. K. Mehta, K. K. Bhasin, R. Chauhan, S. Dham, *Colloids Surf. A.* **2005**, *255*, 153–157.
15. J. Mata, D. Varade, P. Bahadur, *Thermochim. Acta* **2004**, *428*, 147–155.
16. M. L. Free, *Corrosion* **2002**, *58*, 1025–1030.
17. M. L. Free, W. Wang, D.Y. Ryu, *Corrosion* **2004**, *60*, 837–844.
18. M. Hosseini, F. L. Mertens, M. R. Arshadi, *Corros. Sci.* **2003**, *45*, 1473–1489.
19. R. F. V. Villamil, P. Corio, J. C. Rubim, S. M. L. Agostinho, *J. Electroanal. Chem.* **1999**, *472*, 112–119.
20. R. Guo, T. Liu, Wei, *Colloids Surf. A.* **2002**, *209*, 37–45.
21. R. Fuchs-Godec, V. Doleček, *Colloids Surf. A.* **2004**, *244*, 73–76.
22. R. Atkin, V. S. J. Craig, E. J. Walness, S. Biggs, *Adv. in Colloid & Interface Sci.* **2003**, *106*, 219–304.
23. S. Paria, C. Manohar, K. C. Khilar, *Colloids Surf. A.* **2005**, *252*, 221–229.
24. D. P. Schweinsberg, V. Ashworth, *Corros. Sci.* **1988**, *28*, 539–545.
25. R. Fuchs-Godec, *Colloids Surf. A.* **2006**, *280*, 130–139.
26. A. F. Somasundaran, N.J. Turro, *Langmuir* **1997**, *13*, 506–510.
27. T. Behrends, R. Herrmann, *Phys. Chem. Earth.* **1996**, *23*, 2, 229–235.
28. P. Somasundaran, DW Fuerstenau, *J. Phys. Chem.* **1966**, *70*, 90–96.
29. P. Chandar, P. Somasundaran, N. J. Turro, *J. Colloid Interf. Sci.* **1987**, *117*, 31–46.
30. P. Chandar, P. Somasundaran, K. C. Waterman, N. J. Turro, *J. Phys. Chem.* **1987**, *91*, 148–150.
31. P. Somasundaran, C. V. Kunjappu, C. V. Kumar, N. J. Turro, J. K. Barton, *Langmuir* **1989**, *5*, 215–218.
32. E. F. Marques, O.Regev, A. Khan, B. Lindman, *Adv. in Colloid & Interface Sci.* **2003**, *100–102*, 83–104.
33. T. F. Svitova, Y. P. Smirnova, S. A. Pisarev, N. A. Berezina, *Colloids Surf. A.* **1995**, *98*, 107–115.
34. O. Regev, M. S. Leaver, R. Zhou, S. Puntambekar, *Langmuir* **2001**, *17*, 5141–5149.

## Povzetek

S klasično potenciodinamsko metodo smo proučevali inhibitorjski vpliv kvarternih amonijeve soli z različno dolžino oz. številnostjo alkilne verige, ter z različnim protiionom na feritno nerjavno jeklo X4Cr13 v 2 mol L<sup>-1</sup> raztopini žveplove VI. kisline. Izbrani inhibitorji delujejo zaviralno tako na katodne, kot tudi na anodne reakcije. Adsorpcija myristyltrimethylammonijevega klorida (MTACl), myristyltrimethyl-ammonijevegabromida (MTABr), trioctylmethylammonium klorida (TOMACl) in trioctylmethylammonium bromida (TOMABr), je v skladu z Langmuirjevo adsorpcijsko izotermo. Če rišemo  $\log [\theta/(1-\theta)]$  proti  $\log c_{\text{inh}}$  dobimo linearne odvisnosti, za katere je značilno, da se naklon drastično spremeni pri CMC vrednosti za posamezen surfaktant. Odvisnost  $\log \theta$  proti  $\log c_{\text{inh}}$  je v skladu z 'štiri stopenjskim' adsorpcijskim modelom, ki sta ga predlagala Somasundaran in Fuerstenau. V področju nastajanja večslojne plasti (področje IV) smo predpostavili dva različna tipa nastale večslojne plasti v primeru TOMABr in MTABr. Velik vpliv na učinkovitost inhibicije ima dolžina oz. številnost alkilne verige. Le-ta je večji od vpliva protona.